



Article

Photocatalytic H₂O₂ Generation Using Au-Ag Bimetallic Alloy Nanoparticles Loaded on ZnO

Xinzhu Pang ^{1,*}, Nathan Skillen ¹, Detlef W. Bahnemann ^{2,3,4,*} , David W. Rooney ¹ and Peter K. J. Robertson ¹ 

¹ School of Chemistry and Chemical Engineering, Queen's University Belfast, David Keir Building, Stranmillis Road, Belfast BT9 5AG, UK

² Laboratory of Photoactive Nanocomposite Materials, Saint-Petersburg State University, Ulyanovskaya Str. 1, Peterhof, 198504 Saint-Petersburg, Russia

³ School of Environmental Science and Engineering, Shaanxi University of Science and Technology, Xi'an 710021, China

⁴ Institut fuer Technische Chemie, Gottfried Wilhelm Leibniz Universitaet Hannover, Callinstrasse 3, D-30167 Hannover, Germany

* Correspondence: xpang02@qub.ac.uk (X.P.); bahnmann@iftc.uni-hannover.de (D.W.B.)

Abstract: Hydrogen peroxide (H₂O₂) is an important chemical as it is an environmentally friendly oxidant for organic synthesis and environmental remediation as well as a promising candidate for the liquid fuel. Photocatalytic generation of H₂O₂ is sustainable, and many efforts have been put into the development of new catalysts to gain high H₂O₂ yields. In this investigation, Au/ZnO, Ag/ZnO and Au-Ag/ZnO catalysts were prepared by the simultaneous impregnation of HAuCl₄ and AgNO₃ and they were used to generate H₂O₂ from a methanol/O₂ system. It was demonstrated that Au/ZnO had the best performance at generating H₂O₂. The presence of Au on ZnO accelerated the generation of H₂O₂ on ZnO and facilitated H₂O₂ adsorption onto the catalyst surface, which resulted in the reaction kinetics changing from zero-order to first-order. Ag atoms on Ag/ZnO were unstable and would strip from the surface of ZnO during irradiation, decreasing the yield of H₂O₂. The stabilization of Ag on Au-Ag/ZnO depended on the ratio of Au and Ag. Au_{0.1}Ag_{0.2}/ZnO was a stable catalyst and it showed that the presence of Ag promoted the formation and decomposition of peroxide, simultaneously.

Keywords: photocatalysis; oxygen reduction; hydrogen peroxide; Au/ZnO; Au-Ag/ZnO



Citation: Pang, X.; Skillen, N.; Bahnemann, D.W.; Rooney, D.W.; Robertson, P.K.J. Photocatalytic H₂O₂ Generation Using Au-Ag Bimetallic Alloy Nanoparticles Loaded on ZnO. *Catalysts* **2022**, *12*, 939. <https://doi.org/10.3390/catal12090939>

Academic Editor: Giuseppina Luciani

Received: 22 July 2022

Accepted: 16 August 2022

Published: 24 August 2022

Publisher's Note: MDPI stays neutral with regard to jurisdictional claims in published maps and institutional affiliations.



Copyright: © 2022 by the authors. Licensee MDPI, Basel, Switzerland. This article is an open access article distributed under the terms and conditions of the Creative Commons Attribution (CC BY) license (<https://creativecommons.org/licenses/by/4.0/>).

1. Introduction

H₂O₂ is widely used in industry as an oxidant, as it possesses a significant content of active oxygen (47.1 % *w/w*) and emits only water as a by-product [1]. Recently, it has been found that H₂O₂ can act as a clean energy carrier to replace H₂ in fuel cells or even one-compartment cells for the generation of electricity [2]. Moreover, H₂O₂ is easier to store and transport, and has less explosion risk, so H₂O₂ is a promising complementary energy source for the future. Oxidation of anthraquinone is the prevalent process for the industrial production of H₂O₂ but it involves many steps, requires a high energy input and organic solvents and generates solid waste [3]. Many efforts, therefore, have been devoted to developing new methods for H₂O₂ generation which have the potential to be more environmentally friendly.

The application of photocatalysis for the generation of H₂O₂ has gained significant attention since 1988 [4]. This process is conducted in mild conditions (room temperature and atmospheric pressure) and needs only water and oxygen as raw materials, sunlight or UV light as the energy supply, and semiconductors as catalysts [5]. Photocatalytic generation of H₂O₂ on the photocatalyst contains several steps: dissolved oxygen will be adsorbed on the photocatalysts surface; electrons in the valence band (VB) will be excited into the conduction band (CB) when they gain enough energy from the light; e⁻

will react with oxygen on the photocatalyst surface forming H_2O_2 (Equation (1)). TiO_2 is the most frequently-used photocatalyst, and while many researchers have used TiO_2 to generate H_2O_2 , the yields on pure TiO_2 remain low [6]. One of the main reasons that TiO_2 is incapable of stable and sustainable H_2O_2 synthesis via photocatalysis is the formation of peroxy species (Ti-OOH) between the H_2O_2 and TiO_2 , which mediates the decomposition of H_2O_2 [7]. Loading novel metal particles onto TiO_2 (e.g., Pt, Pd, Au) is an efficient way to improve the photocatalytic production of H_2O_2 and some studies have shown that irradiation of the metal/ TiO_2 photocatalysts with UV light in an O_2 -saturated ethanol/water mixture can produce significantly more H_2O_2 [8,9]. The presence of Au on TiO_2 has been found to increase production of H_2O_2 as a result of the increased electron transfer from TiO_2 to Au through a Schottky junction, and led to an increase in the two-electron reduction of O_2 (Equation (1)) [10]. Some researchers have investigated the effect of loading two metals, such as Au and Ag onto TiO_2 to promote the H_2O_2 formation [11].



Graphite-like carbon nitride ($\text{g-C}_3\text{N}_4$) is a metal free polymer n-type semiconductor, and it is seen as a potential candidate to produce H_2O_2 [12]. Even though the photocatalytic activity of $\text{g-C}_3\text{N}_4$ is still low, many efforts have proven to be successful at promoting H_2O_2 yield. For example, Li et al., introduced carbon vacancies on $\text{g-C}_3\text{N}_4$ and those vacancies helped it generate more H_2O_2 [13]. Additionally, various other inorganic-based photocatalysts have also been explored for the generation of H_2O_2 . Hirakawa et al., investigated the performance of bismuthvanadate (BiVO_4) to generate H_2O_2 under visible light [14]. Another common commercial photocatalyst, ZnO, has been reported to result in higher H_2O_2 yields compared to TiO_2 [4]. There have however been fewer investigations into the effect of metal loading onto the surface of ZnO for H_2O_2 production. Meng et al. [15] synthesised an Au/ZnO material and found that H_2O_2 yields on Au/ZnO were significantly higher compared to those obtained on Au/ TiO_2 . Kawano et al., [16] subsequently reported that the enhanced performance of Au/ZnO for generation of H_2O_2 was a result of both effective charge separation and the lower adsorptivity of H_2O_2 to the surface of catalysts. There has been little research performed around the loading of alloys on ZnO to generate H_2O_2 .

In this paper, the assessment of bimetallic loaded ZnO photocatalysts for H_2O_2 production is reported. Au-Ag/ZnO catalysts with alloy particles consisting of Au and Ag were prepared by simultaneous impregnation of HAuCl_4 and AgNO_3 . Au/ZnO and Ag/ZnO were also made using the same methods. For comparison, P25 TiO_2 with the same loadings were prepared and their efficiency for H_2O_2 generation was also tested.

2. Results and Discussion

2.1. Characterization of Catalysts

A typical SEM_EDX image of $\text{Au}_{0.1}\text{Ag}_{0.4}/\text{ZnO}$ is shown in Figure 1a. From the SEM image of the $\text{Au}_{0.1}\text{Ag}_{0.4}/\text{ZnO}$ material the particle size was determined to be 309 nm. Energy dispersive X-ray spectroscopy (EDX) of metal particles on the catalyst determined the average Au/Ag ratio as 0.16 (mol/mol). The XRD pattern of ZnO and $\text{Au}_{0.1}\text{Ag}_{0.4}/\text{ZnO}$ is shown in Figure 1b. The exact amount of Au and Ag on the ZnO photocatalyst was determined by Inductively coupled plasma—optical emission spectrometry (ICP-OES) and was found to be 0.21 (mol/mol). The EDX also shows that the Au and Ag components in the metal particles were mixed homogeneously (not shown in the manuscript). The Ag and Au loadings and particle size of the modified ZnO and TiO_2 materials are summarized in Table 1.

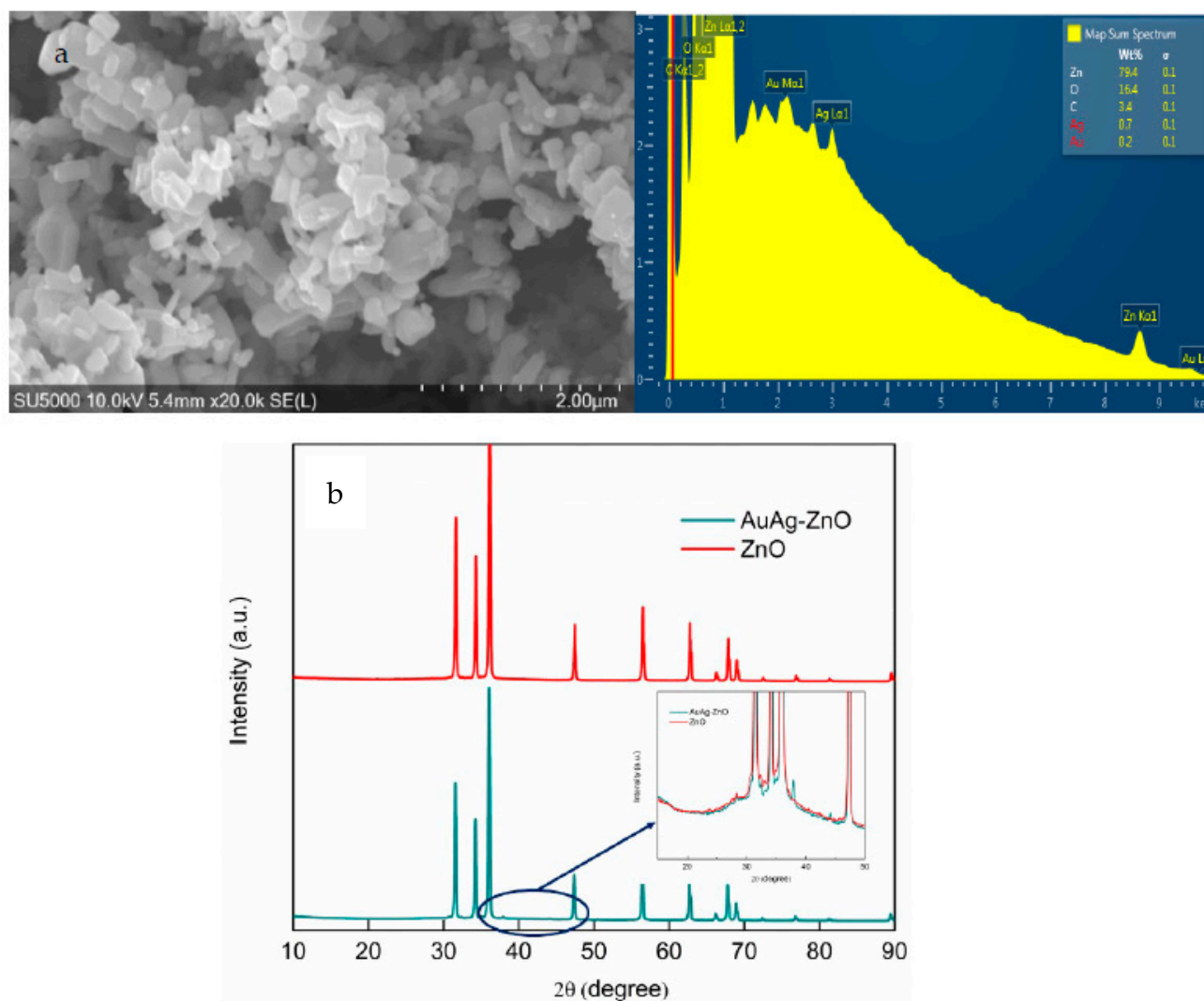


Figure 1. (a) Typical SEM_EDX image of Au_{0.1}Ag_{0.4}/ZnO; (b) XRD pattern of ZnO Au_{0.1}Ag_{0.4}/ZnO nanoparticle.

Table 1. Summary of metal loadings on catalysts.

| | Au Content/mol% ^a | Ag Content/mol% ^a | Particle Size/nm |
|---|------------------------------|------------------------------|------------------|
| Au _{0.1} Ag _{0.4} /ZnO | 0.14 | 0.68 | 309 |
| Au _{0.1} Ag _{0.4} /TiO ₂ | 0.14 | 0.73 | 65 |
| Au _{0.1} /ZnO | 0.15 | - | 411 |
| Au _{0.2} /ZnO | 0.26 | - | |
| Au _{0.3} /ZnO | 0.37 | - | |
| Ag _{0.2} /ZnO | - | 0.27 | 235 |
| Ag _{0.2} /ZnO ^b | | 0.14 | |

(a): amount of Au and Ag was determined by ICP-OES; (b): catalyst recovered after 1 h reaction.

The UV–vis spectra of the metal modified ZnO photocatalyst materials are shown in Figure 2. As shown, adding Au onto ZnO enabled the catalysts to adsorb photons in the visible portion of light. This work, however, focused on the photocatalytic generation of H₂O₂ under UV light.

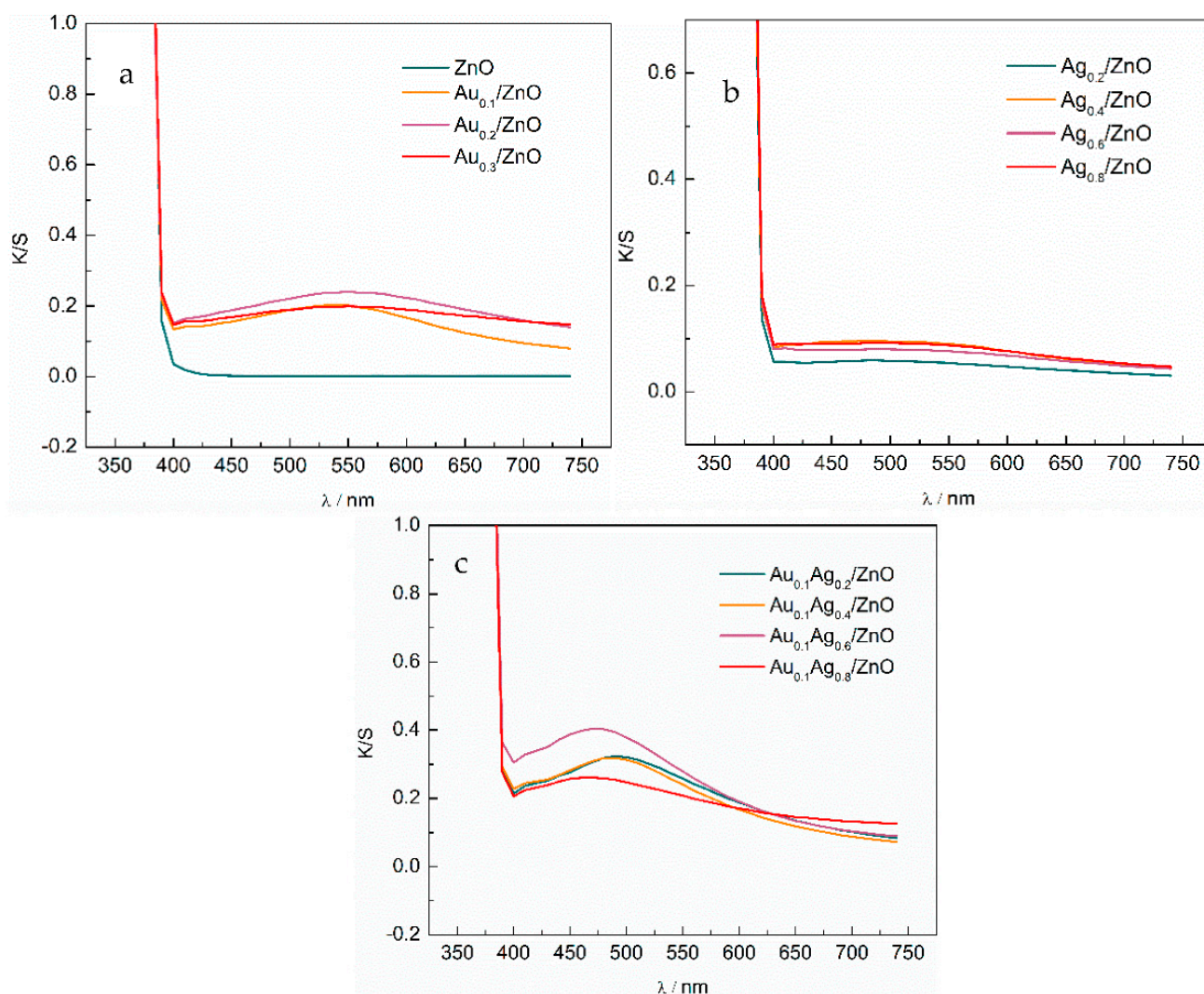


Figure 2. Diffuse reflectance UV-vis spectra of respective catalysts (a): ZnO and Au/ZnO; (b): Ag/ZnO; (c): Au-Ag/ZnO.

2.2. Photocatalytic Generation of H₂O₂

The photocatalytic activity of H₂O₂ generation on catalysts was tested under UV light by adding 50 mg of photocatalyst into 100 mL 0.1 M methanol solution. Methanol reacts with h⁺ on the CB, replacing water as the electron donor and, due to its lower oxidation potentials and faster reaction kinetics, strongly inhibits other oxidation processes [6]. Formaldehyde was also detected in the system and was found to increase linearly during the reaction (not shown in the manuscript). At the same time, oxygen was reduced on the CB to form H₂O₂.

After one hour of UV illumination, the yield of H₂O₂ was recorded, Figure 3. It showed that when the Au loading changed from 0 to 0.2 mol%, the H₂O₂ yield increased from 1117.91 μ M to 1281.93 μ M. When the Au loading was further increased to 0.3 mol%, the H₂O₂ yield decreased to 1266.59 μ M. Previous research also reported that a loading of 0.1 mol% Au on ZnO facilitated an increased generation of H₂O₂ compared to bare ZnO [15].

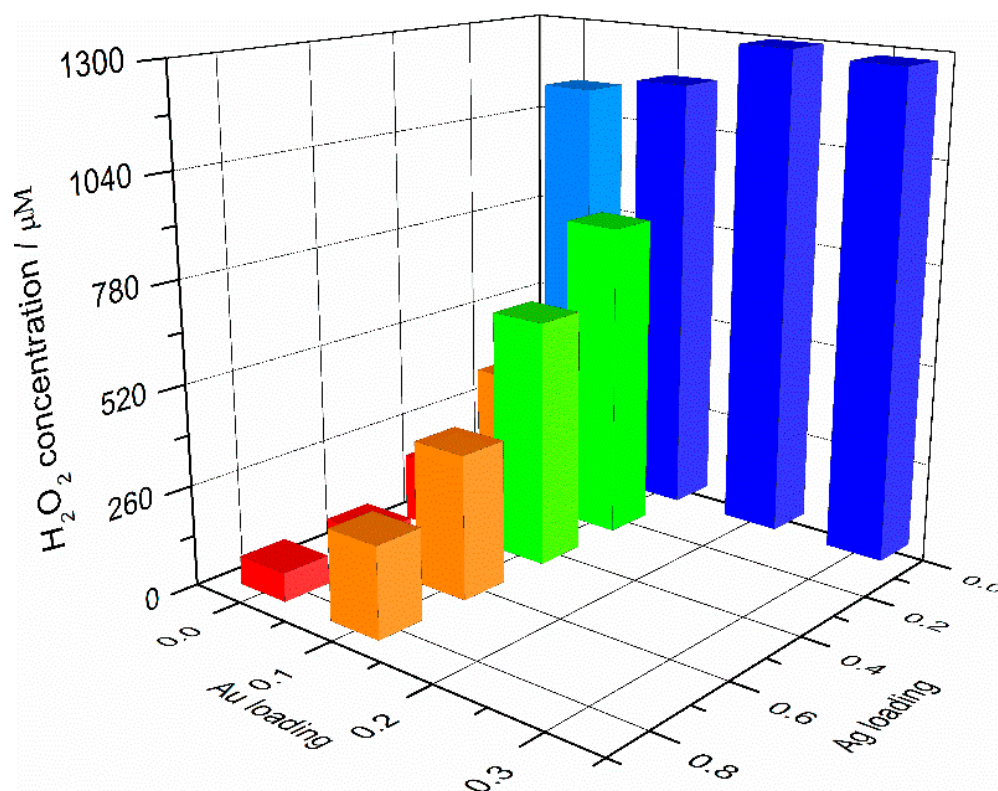


Figure 3. H₂O₂ yield on ZnO loaded photocatalyst after one hour illumination (50 mg catalyst in 100 mL 0.1 M methanol solution).

Au loading on photocatalysts is believed to enhance H₂O₂ generation as a result of reduced recombination in ZnO particles occurring, due to the transfer of photoexcited electrons to the metal nanoparticles [17]. The charge separation is effectively assisted by the interfacial electron transfer from the CB of ZnO (e^-_{CB}) to Au (e^-_{Au}) [8]. The accumulated electrons (both e^-_{CB} and e^-_{Au}) on the catalysts, however, decompose H₂O₂. If H₂O₂ was not adsorbed onto the catalyst, however, it would not be decomposed by electrons, as demonstrated on bare ZnO. It was found that H₂O₂, however, can adsorb onto the Au/ZnO surface (adsorption of H₂O₂ on modified ZnO will be illustrated in Section 2.3) and thus can be decomposed through the reduction reaction with e^- (Equation (2)) [18,19]. This illustrated that Au particles could promote the simultaneous formation and decomposition of H₂O₂, in a similar manner to what happens with TiO₂ materials.



From Figure 3, it can be seen that when Ag was loaded on ZnO, the H₂O₂ yield decreased significantly with increasing Ag loading. Specifically, when Ag loading increased from 0 to 0.8 mol%, the H₂O₂ yield decreased from 1117.91 µM to 74.18 µM. When both Au and Ag were loaded onto ZnO, and the metal loading changed from Au_{0.1}Ag_{0.2} to Au_{0.1}Ag_{0.8}, the H₂O₂ yield decreased from 824.27 µM to 234.77 µM. This observation may be explained by the fact that Ag particles on ZnO promoted significant adsorption of H₂O₂ to the photocatalyst surface (the effect of adsorption is described in Section 2.3). Furthermore, photoexcited electrons from the ZnO photocatalyst may also be trapped on the surface of the Ag atoms, which would subsequently decompose the H₂O₂ (Equation (2)). Another reason for the lower levels of H₂O₂ generation on Ag/ZnO may be that the Ag on Ag/ZnO was not stable and this again is illustrated in Section 2.3.

Photocorrosion of ZnO has previously been extensively reported in the literature, and this process not only required UV irradiation, but also resulted from the photocatalytic reaction [20]. The photostability of ZnO was also assessed in this study and the results are

summarized in Table 2. The solution was filtered after the reaction and the concentration of Zn^{2+} was determined using ICP. Accordingly, the loss of catalyst can be calculated, which was determined to be 0.97%. The loss of Zn on Ag/ZnO and Au/ZnO was 0.74% and 1.63%, respectively. As the amount of catalyst loss was minimal, it was considered negligible. On the other hand, this data also illustrated that the loading of Au helped to improve the photostability of ZnO, while the loading of Ag decreased the photostability of ZnO.

Table 2. The photocorrosion of different ZnO catalyst.

| | ZnO | Au _{0.2} /ZnO | Ag _{0.2} /ZnO | Au _{0.1} Ag _{0.2} /ZnO |
|-------------------------------------|------|------------------------|------------------------|--|
| Zn ²⁺ after reaction/ppm | 3.9 | 3.0 | 6.5 | 3.3 |
| ZnO loss/% | 0.97 | 0.74 | 1.63 | 0.82 |

For a comparison with the ZnO materials, TiO₂ catalysts with the same metal loadings were prepared and used for the generation of H₂O₂ under the same conditions. The results from the study of the metal modified TiO₂ for generation of H₂O₂ are summarized in Figure 4. When pure TiO₂ was used, approximately 10 μM H₂O₂ was generated (red bar in Figure 4), which was significantly lower than the ZnO catalysts. When Au and Ag were loaded on TiO₂, the yield of H₂O₂ increased from 40 μM to 130 μM depending on metal loadings. These results suggested that loading with both Au and Ag metals promotes two-electron reduction of O₂ and hence facilitates H₂O₂ production. It was observed (Figure 4) that when only Au was loaded onto TiO₂, the Au_{0.2}/TiO₂ material showed the best photocatalytic activity (79.26 μM) and when only Ag was loaded onto TiO₂, Ag_{0.4}/TiO₂ demonstrated the best activity for H₂O₂ generation (111.13 μM). Comparison of Au-Ag bimetallic catalysts demonstrated that Au_{0.1}Ag_{0.2}/TiO₂ was the best material at generating H₂O₂ (133.22 μM).

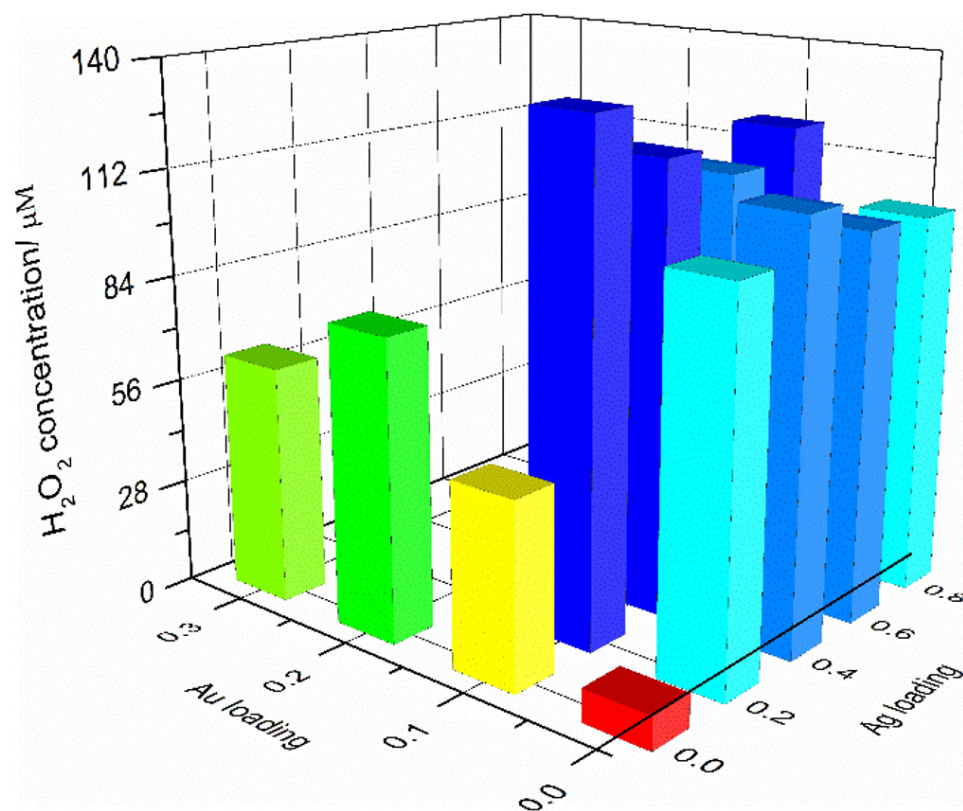


Figure 4. H₂O₂ yield on modified TiO₂ after one hour illumination (50 mg catalyst in 100 mL 0.1 M methanol solution).

It is important to note that with the same metal loading, compared with the modified TiO₂ photocatalyst, modified ZnO generated almost one order of magnitude higher yields of H₂O₂. Specifically, Au_{0.1}Ag_{0.2}/TiO₂ generated the most H₂O₂ which was only 133.22 μM, while the yield on Au_{0.2}/ZnO was 1281.93 μM.

2.3. Kinetics of H₂O₂ Formation on Modified ZnO

The time-concentration profiles of the photocatalytic generation of H₂O₂ on ZnO with different Au loadings are summarized in Figure 5.

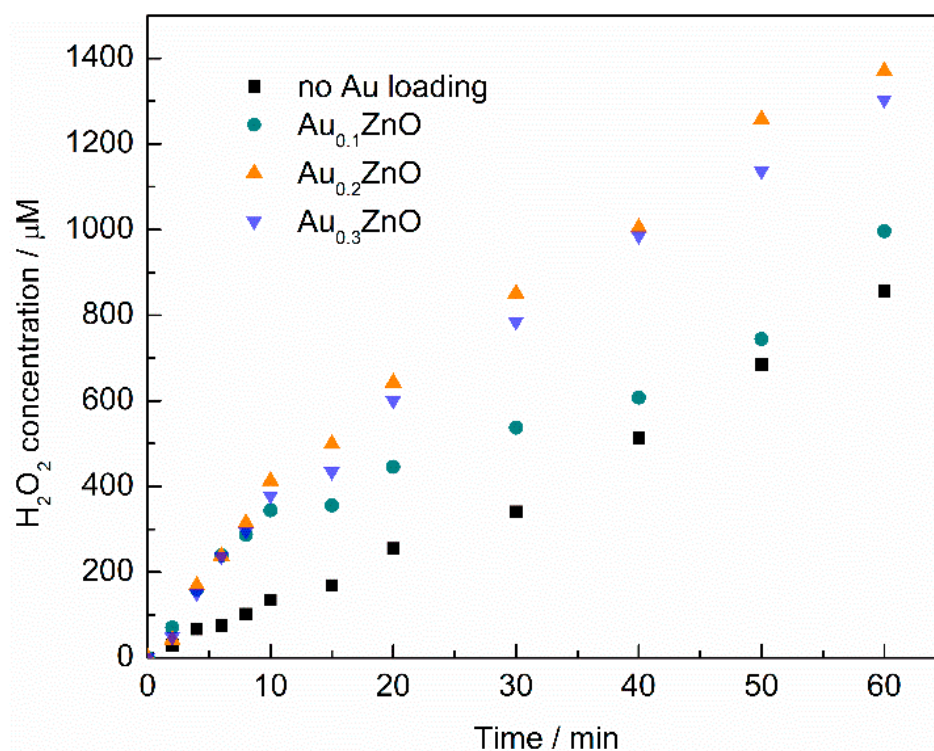


Figure 5. Time-concentration profile of H₂O₂ generation on different Au-ZnO.

The rates for formation and decomposition of H₂O₂ on TiO₂ follow zero- and first-order kinetics toward H₂O₂ concentration, respectively (Equations (3) and (4)) [6]. Combining Equations (3) and (4), the profile of $c(\text{H}_2\text{O}_2)$ and time can be described in Equation (5). Considering $[\text{H}_2\text{O}_2]_0 = 0$, in this case, the Equation (5) can be simplified into Equation (6) [6].

$$r_F = \Phi_F I_{\text{abs}} = k_F \quad (3)$$

$$r_D = \Phi_D [\text{H}_2\text{O}_2] I_{\text{abs}} = k_D [\text{H}_2\text{O}_2] \quad (4)$$

$$[\text{H}_2\text{O}_2] = \frac{k_F}{k_D} (1 - e^{-k_D t}) + [\text{H}_2\text{O}_2]_0 \cdot e^{-k_D t} \quad (5)$$

$$[\text{H}_2\text{O}_2] = \frac{k_F}{k_D} (1 - e^{-k_D t}) \quad (6)$$

The generation of H₂O₂ on pure ZnO followed zero-order reaction kinetics ($k_D \approx 0$), which has previously been reported by others [4]. This is believed to be due to the fact that the photocatalytically generated H₂O₂ does not adsorb onto the surface of the unmodified ZnO photocatalyst (black square in Figure 5) [21]. When Au was loaded onto the ZnO material, the kinetics for H₂O₂ generation were observed to change to a first-order process. In this case the Au particles on the ZnO surface allowed adsorption of H₂O₂. The specific influence of Au loading on the adsorption of H₂O₂ will be discussed below. From these

results it can be seen that H_2O_2 was generated quickly (within 1 h) on the Au/ZnO photocatalyst. During irradiation, however, the generation rate of H_2O_2 on Au/ZnO became slower, and consequently the yield of H_2O_2 on unmodified ZnO was expected to surpass that of the Au/ZnO material at some point. In Figure 5, the yield of H_2O_2 on unmodified ZnO was almost the same as that observed for the $\text{Au}_{0.1}/\text{ZnO}$ material, while the H_2O_2 yield on the unmodified ZnO surpassed that observed for the $\text{Au}_{0.1}/\text{ZnO}$ photocatalyst following 2 hours illumination.

As the kinetics of H_2O_2 generation follow first-order profiles for the modified materials, the generation rate constant (k_F) and decomposition rate constant (k_D) could be calculated from Equation (6). Parameter k_F explains the ability to generate H_2O_2 while parameter k_D demonstrates the ability to degrade H_2O_2 on the surface of catalysts. The apparent quantum yield or photonic efficiency (ξ) was calculated from Equations (7)–(8). Accordingly, k_F and k_D and photonic efficiencies on different Au loadings are summarized in Table 3.

Table 3. Summary of k_F , k_D and ξ of different Au/ZnO during H_2O_2 generation.

| Au Loading | 0 | 0.1 mol% | 0.2 mol% | 0.3 mol% |
|---|---------|----------|----------|----------|
| Yield after 1 h illumination/ μM | 1117.97 | 1160.00 | 1281.93 | 1266.59 |
| $k_F/\mu\text{M min}^{-1}$ | 18.633 | 23.496 | 33.213 | 32.586 |
| k_D/min^{-1} | 0 | 0.0137 | 0.0118 | 0.0134 |
| $\xi/\%$ | 3.41 | 4.30 | 6.08 | 5.97 |

From Table 3 it can be seen that k_F for $\text{Au}_{0.2}/\text{ZnO}$ ($33.213 \mu\text{M min}^{-1}$) was higher than that for different Au loadings and at the same time, its k_D was lower than the other modified catalysts. This would suggest that all three of these Au loadings are effective in promoting H_2O_2 formation. This data indicated that Au particles on ZnO facilitated both the formation and decomposition of H_2O_2 .

To determine the adsorption of H_2O_2 on the photocatalysts, 50 mg of photocatalyst was added to 100 mL 1000 μM H_2O_2 and stirred in the dark for one hour. The percentage of H_2O_2 adsorbed onto modified ZnO is summarized in Figure 6. On bare ZnO, no adsorption of H_2O_2 was observed. After one-hour dark adsorption, the concentration of H_2O_2 increased slightly, which may be due to water evaporation. Upon modifying the ZnO materials with Ag, it was observed that the percentage of H_2O_2 adsorbed onto the photocatalyst increased with increasing Ag loading. When Ag loadings changed from 0 to 0.8 mol%, the percentage of H_2O_2 adsorbed onto the catalyst increased from -3.74% to 38.48% . The loading of Au onto ZnO materials also facilitated H_2O_2 adsorption, with greater loading of Au resulting in higher levels of H_2O_2 adsorption. As Au loadings increased from 0 to 0.3 mol%, the percentage of H_2O_2 adsorbed onto the photocatalyst increased from -3.74% to 7.94% . The Au loading, however, did not promote H_2O_2 adsorption as strongly as Ag loadings. For the same 0.2 mol% metal loading, $\text{Au}_{0.2}/\text{ZnO}$ and $\text{Ag}_{0.2}/\text{ZnO}$ adsorbed 5.58% and 8.66% H_2O_2 , respectively. On the Au-Ag Bimetallic catalyst, H_2O_2 adsorption was enhanced significantly. For example, 57.65% H_2O_2 was adsorbed onto the $\text{Au}_{0.1}\text{Ag}_{0.8}/\text{ZnO}$ catalyst (Figure 6).

These results showed that with greater Au loadings, the Au/ZnO photocatalyst materials would adsorb more of the photocatalytically generated H_2O_2 onto its surface, which would in turn would promote the decomposition of the H_2O_2 .

The time-concentration profiles of the photocatalytic H_2O_2 generation on Ag/ZnO are summarized in Figure 7a. From this figure it can be seen that the concentration of H_2O_2 increased sharply during the first 5 min to around $250 \mu\text{M}$ and then it dropped off until 20 min of photocatalysis, after which the concentration of H_2O_2 starts to increase again. Additionally, increasing yields of H_2O_2 were obtained after 120 min of photocatalysis as Ag loadings decrease. For example, when the Ag loading increased from 0.2% mol to 0.8% mol, the yield dropped from $1082.57 \mu\text{M}$ to $225.29 \mu\text{M}$. This would suggest that the Ag/ZnO was not a stable catalyst with this simultaneous impregnation of HAuCl_4 and AgNO_3 method.

It was assumed that Ag atoms may separate from the surface of the catalyst. Table 1 showed that following the photocatalytic reaction, the amount of Ag in $\text{Ag}_{0.2}/\text{ZnO}$ decreased from 0.27% to 0.14%. Additionally, EDX detected the presence of Ag on $\text{Ag}_{0.2}/\text{ZnO}$, while it did not detect the presence of Ag on the $\text{Ag}_{0.2}/\text{ZnO}$ material which had been used in a photocatalytic reaction. It is proposed that the Ag metals which shed from the ZnO surface could decompose H_2O_2 in the solution or the Ag particles could also adsorb H_2O_2 onto their surface, hence decreasing the concentration of H_2O_2 in the aqueous solution.

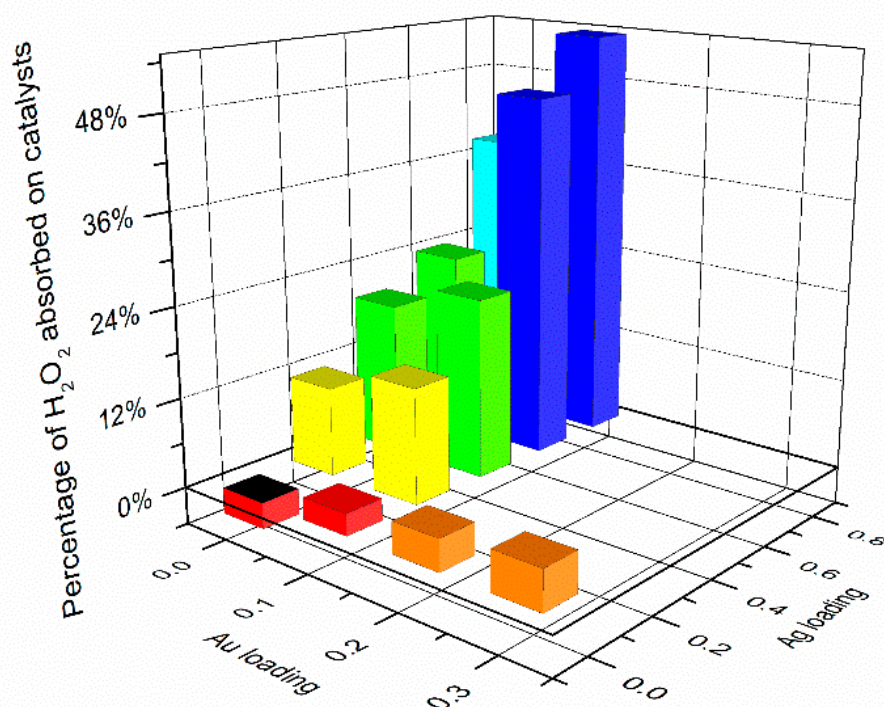


Figure 6. Percentage of H_2O_2 adsorbed on modified ZnO after 1 h dark stirring (50 mg catalysts in 100 mL 1000 μM H_2O_2 solution).

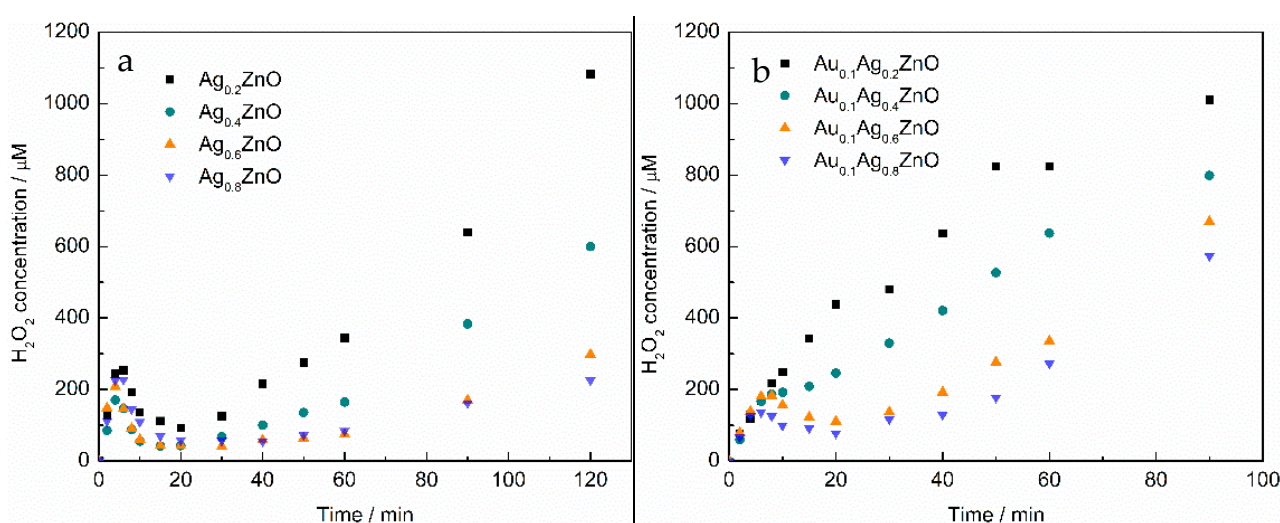


Figure 7. (a), Time-concentration profile of generation of H_2O_2 on Ag/ZnO . (b), Time-concentration profile of generation of H_2O_2 on $\text{Au-Ag}/\text{ZnO}$.

The time-concentration profiles of the photocatalytic generation of H_2O_2 on different $\text{Au-Ag}/\text{ZnO}$ materials are summarized in Figure 7b. This figure shows that when both Au

and Ag were loaded onto ZnO, the presence of Au helped to stabilize the Ag atoms. For $\text{Au}_{0.1}\text{Ag}_{0.8}/\text{ZnO}$, the generation of H_2O_2 increased during the first 5 min of photocatalysis, then the yield decreased until 20 min of irradiation before starting to increase again. The yield had declined at 20 min of photocatalysis time by 45%, compared to that observed at 5 min of irradiation time (from 136.41 μM to 77.29 μM). On $\text{Ag}_{0.8}/\text{ZnO}$, however, this decrease was much greater at approximately 75% (from 227.03 μM to 57.74 μM). The level of decline in H_2O_2 generation during the photocatalytic process was found to increase with increasing Ag loadings. Interestingly, the $\text{Au}_{0.1}\text{Ag}_{0.2}/\text{ZnO}$ material was proved to be a stable catalyst for peroxide production, with the generation of H_2O_2 not following the 'first rise and then fall' pattern observed with other materials. This material followed the first-order kinetic profile and the k_F and k_D of H_2O_2 on $\text{Au}_{0.1}\text{Ag}_{0.2}/\text{ZnO}$ were calculated as 25.056 $\mu\text{M min}^{-1}$ and 0.021 min^{-1} using Equation (6). The corresponding k_F and k_D values for $\text{Au}_{0.1}/\text{ZnO}$ were 23.496 $\mu\text{M min}^{-1}$ and 0.014 min^{-1} . It is assumed that the inclusion of the Au atoms could stabilise the Au-Ag/ZnO material. Compared with $\text{Au}_{0.1}/\text{ZnO}$, higher k_F and higher k_D were observed that demonstrated that the presence of Ag could promote the formation and decomposition of H_2O_2 simultaneously. It should be noted that if Au-Ag/ZnO is going to be further explored for H_2O_2 production, the ratio of Au/Ag should be carefully monitored.

3. Materials and Methods

3.1. Materials

TiO_2 P25 (80% Anatase and 20% Rutile) and ZnO were purchased from Evonik Aeroxide and Fisher Chemical, respectively. $\text{HAuCl}_4 \cdot 3\text{H}_2\text{O}$ and AgNO_3 were purchased from Sigma Aldrich. Syringe filters (0.22 μm) were purchased from Merck Millipore Ltd. Fluorescent reagent contained POHPAA (8 mg, Tokyo Chemical Industry) and lyophilized powder of HRP (2 mg, Alfa Aesar), which were both dissolved in TRIS buffer (25 mL, 1.0 M, pH 8.8, Alfa Aesar). A Millipore Waters Milli-Q purification unit was used to provide ultrapure water (18.2 $\text{M}\Omega/\text{cm}$) in all experiments. A UV-LED (Series ILH-Xx01-Sxxx-SC211-WIR200, Intelligent LED Solutions) with a peak wavelength at 370 nm and 65° viewing angle was used ($I = 0.25$ A and $V = 14$ V). Potassium ferrioxalate was purchased from Alfa Aesar.

3.2. Preparation of Photocatalyst

TiO_2 (1.0 g) or ZnO (1.019 g) was added to water (50 mL) containing $\text{HAuCl}_4 \cdot 3\text{H}_2\text{O}$ (5.6 mg) and AgNO_3 (1.6, 3.9, 7.9, 11.9, or 15.9 mg). The pH of solution was adjusted to about 7 with a NaOH solution (1 mM), and water was evaporated at 80 °C with stirring. The powders were dried at 100 °C for 12 h, calcined in air at 400 °C for 2 h, and reduced with 5% H_2 at 500 °C for 3 h, affording $\text{Au}_{0.1}\text{Ag}_y/\text{TiO}_2$ ($y = 0.1, 0.2, 0.4, 0.6, 0.8$) and $\text{Au}_{0.1}\text{Ag}_y/\text{ZnO}$ ($y = 0.1, 0.2, 0.4, 0.6, 0.8$). Au_x/TiO_2 ($x = 0.1, 0.2, 0.3$), Au_x/ZnO ($x = 0.1, 0.2, 0.3$), Ag_y/TiO_2 ($y = 0.2, 0.4, 0.6, 0.8$), Ag_y/ZnO ($y = 0.2, 0.4, 0.6, 0.8$) catalysts were prepared in a similar manner using AgNO_3 , $\text{HAuCl}_4 \cdot 3\text{H}_2\text{O}$ as metal precursors.

3.3. Photocatalytic Generation of H_2O_2

Catalyst (50 mg) was suspended in 100 mL 0.1 M methanol solution and stirred continually with a magnetic stirrer. Samples were taken from the reaction solution and filtered through a syringe filter (0.22 μm). The H_2O_2 concentration of the samples were analysed using the horseradish peroxidase (HRP)-catalyzed stoichiometric dimerization of p-hydroxyphenylacetic acid (POHPAA) method which yields a fluorescent product ($\lambda_{\text{ex}} = 315$ nm, $\lambda_{\text{em}} = 406$ nm) [11]. A sample (2 mL) containing H_2O_2 (diluted if needed), and 0.25 mL fluorescent solution were analysed by a luminescence spectrometer fluorimeter (PerkinElmer LS 50 B Luminescence Spectrometer Fluorimeter) after 30 min reaction ($\lambda_{\text{ex}} = 315$ nm, $\lambda_{\text{em}} = 406$ nm). The concentration of H_2O_2 was calculated from a calibration of known H_2O_2 concentrations.

The photon flux was determined using the potassium ferrioxalate actinometrical method and by replacing the photocatalytic solution with actinometry solution under the same conditions of H₂O₂ generation, Equation (7) [22].

$$\text{Photonic flux} = \frac{\text{Fe}^{2+}}{\sigma\text{Fe}^{2+} \times t} \quad (7)$$

σFe^{2+} was set at 0.97 and t was the time (min) the actinometry solution was irradiated for. In this system, photon flux was calculated as $1.092 \times 10^{-4} \text{ mol min}^{-1}$ and the photon flux density was then $1.092 \times 10^{-3} \text{ M min}^{-1}$ accordingly. The photonic efficiency was then determined based on Equation (8) [6].

$$\xi (\%) = \frac{2 k_F}{\text{Photon flux density}} \times 100 \quad (8)$$

where ξ (%) is the photonic efficiency, k_F is the H₂O₂ formation rate (M min^{-1}). As the H₂O₂ formation is a 2-electron step, the k_F was multiplied by 2.

3.4. Adsorption of H₂O₂ on Catalysts

To determine the adsorption of H₂O₂ on the photocatalysts, 50 mg photocatalyst was put in 100 mL 1000 μM H₂O₂ solution and stirred in the dark for 60 min. Samples were taken from the solution and filtered through a syringe filter (0.22 μm) and the concentration of H₂O₂ was determined as detailed above.

3.5. Characterization of Photocatalyst

The scanning electron microscope (SEM) was a Field Emission Hitachi SU5000. The accelerating voltage is stated on image (10 kV was used for all images) and analysis was conducted under high vacuum pressure of $\sim 10^{-8}$ bar. The SEM was equipped with a dispersive energy X-ray (EDX/EDS) analyser and conducted with an accelerating voltage of 10 kV. The images were recorded with a backscattered secondary electron detector and performed with the Aztec software provided with the instrument. The EDX was used to confirm the presence of Au and Ag. The particle size of the catalysts was obtained from the SEM figure. The exact amounts of Au and Ag in the catalysts were determined by inductively coupled plasma-optical emission spectrometry (ICP-OES). Diffuse reflectance UV-vis spectra were measured on a UV-vis spectrophotometer (KONICA MINOLTA SENSING, INC. CM-2500d) with BaSO₄ as a reference. XRD data was recorded in Bruker AXS, 5465 East Cheryl Parkway, USA (40 kV, 25 mA).

4. Conclusions

In this paper, Au/ZnO, Ag/ZnO and Au-Ag/ZnO catalysts were prepared by simultaneous impregnation of HAuCl₄ and AgNO₃ and their ability to generate H₂O₂ in a methanol/O₂ system was assessed. The results showed that the Au_{0.2}/ZnO material generated the greatest quantities of H₂O₂ after one hour illumination. The presence of Au on ZnO resulted in greater quantities of H₂O₂ being adsorbed onto the photocatalysts compared to the unmodified ZnO material. This resulted in the kinetics for H₂O₂ generation changing from zero-order for the unmodified material to first-order reaction for the Au/ZnO materials. Ag atoms on Ag/ZnO were found to be unstable and separated from the surface of ZnO during irradiation, also resulting in decreasing yields of H₂O₂. The stabilization of Ag on Au-Ag/ZnO was believed to have been improved due to the presence of Au particles. While Au_{0.1}Ag_{0.2}/ZnO was a stable catalyst, the generation of H₂O₂ was not as high as that on Au_{0.1}/ZnO, as the presence of Ag in the Au-Ag/ZnO material promoted the formation and decomposition of H₂O₂, simultaneously.

Author Contributions: Conceptualization, X.P.; methodology, X.P., N.S., D.W.B., D.W.R. and P.K.J.R.; formal analysis, X.P., D.W.B., N.S. and P.K.J.R.; writing—original draft preparation, X.P.; writing—review and editing, P.K.J.R., D.W.B. and N.S.; supervision, P.K.J.R., D.W.R., N.S. and D.W.B. All authors have read and agreed to the published version of the manuscript.

Funding: X.P. is grateful to acknowledge financial support from the China Scholarship Council (No. 201806030133) for funding her PhD research.

Conflicts of Interest: The authors declare no conflict of interest.

References

1. Sato, K.; Aoki, M.; Noyori, R. A “green” route to adipic acid: Direct oxidation of cyclohexenes with 30 percent hydrogen peroxide. *J. Sci.* **1998**, *281*, 1646–1647. [[CrossRef](#)]
2. Kofuji, Y.; Isobe, Y.; Shiraishi, Y.; Sakamoto, H.; Tanaka, S.; Ichikawa, S.; Hirai, T. Carbon Nitride-Aromatic Diimide-Graphene Nanohybrids: Metal-Free Photocatalysts for Solar-to-Hydrogen Peroxide Energy Conversion with 0.2% Efficiency. *J. Am. Chem. Soc.* **2016**, *138*, 10019–10025. [[CrossRef](#)] [[PubMed](#)]
3. Campos-Martin, J.M.; Blanco-Brieva, G.; Fierro, J.L.G. Hydrogen peroxide synthesis: An outlook beyond the anthraquinone process. *Angew. Chem. Int. Ed.* **2006**, *45*, 6962–6984. [[CrossRef](#)] [[PubMed](#)]
4. Kormann, C.; Bahnemann, D.W.; Hoffmann, M.R. Photocatalytic production of H₂O₂ and organic peroxides in aqueous suspensions of TiO₂, ZnO, and desert sand. *Environ. Sci. Technol.* **1988**, *22*, 798–806. [[CrossRef](#)] [[PubMed](#)]
5. Hou, H.; Zeng, X.; Zhang, X. Production of Hydrogen Peroxide by Photocatalytic Processes. *Angew. Chem. Int. Ed.* **2020**, *59*, 17356–17376. [[CrossRef](#)]
6. Burek, B.O.; Bahnemann, D.W.; Bloh, J.Z. Modeling and Optimization of the Photocatalytic Reduction of Molecular Oxygen to Hydrogen Peroxide over Titanium Dioxide. *ACS Catal.* **2019**, *9*, 25–37. [[CrossRef](#)]
7. Hasnat, M.A.; Uddin, M.M.; Samed, A.J.F.; Alam, S.S.; Hossain, S. Adsorption and photocatalytic decolorization of a synthetic dye erythrosine on anatase TiO₂ and ZnO surfaces. *J. Hazard. Mater.* **2007**, *147*, 471–477. [[CrossRef](#)]
8. Teranishi, M.; Naya, S.I.; Tada, H. Temperature- and pH-Dependence of Hydrogen Peroxide Formation from Molecular Oxygen by Gold Nanoparticle-Loaded Titanium(IV) Oxide Photocatalyst. *J. Phys. Chem. C* **2016**, *120*, 1083–1088. [[CrossRef](#)]
9. Zuo, G.; Li, B.; Guo, Z.; Wang, L.; Yang, F.; Hou, W.; Zhang, S.; Zong, P.; Liu, S.; Meng, X.; et al. Efficient Photocatalytic Hydrogen Peroxide Production over TiO₂ Passivated by SnO₂. *Catalysts* **2019**, *9*, 623. [[CrossRef](#)]
10. Teranishi, M.; Naya, S.I.; Tada, H. In situ liquid phase synthesis of hydrogen peroxide from molecular oxygen using gold nanoparticle-loaded titanium(IV) dioxide photocatalyst. *J. Am. Chem. Soc.* **2010**, *132*, 7850–7851. [[CrossRef](#)]
11. Tsukamoto, D.; Shiro, A.; Shiraishi, Y.; Sugano, Y.; Ichikawa, S.; Tanaka, S.; Hirai, T. Photocatalytic H₂O₂ production from ethanol/O₂ system using TiO₂ loaded with Au-Ag bimetallic alloy nanoparticles. *ACS Catal.* **2012**, *2*, 599–603. [[CrossRef](#)]
12. Shiraishi, Y.; Kofuji, Y.; Sakamoto, H.; Tanaka, S.; Ichikawa, S.; Hirai, T. Effects of Surface Defects on Photocatalytic H₂O₂ Production by Mesoporous Graphitic Carbon Nitride under Visible Light Irradiation. *ACS Catal.* **2015**, *5*, 3058–3066. [[CrossRef](#)]
13. Li, S.; Dong, G.; Hailili, R.; Yang, L.; Li, Y.; Wang, F.; Zeng, Y.; Wang, C. Effective photocatalytic H₂O₂ production under visible light irradiation at g-C₃N₄ modulated by carbon vacancies. *Appl. Catal. B Environ.* **2016**, *190*, 26–35. [[CrossRef](#)]
14. Hirakawa, H.; Shiota, S.; Shiraishi, Y.; Sakamoto, H.; Ichikawa, S.; Hirai, T. Au Nanoparticles Supported on BiVO₄: Effective Inorganic Photocatalysts for H₂O₂ Production from Water and O₂ under Visible Light. *ACS Catal.* **2016**, *6*, 4976–4982. [[CrossRef](#)]
15. Meng, X.; Zong, P.; Wang, L.; Yang, F.; Hou, W.; Zhang, S.; Li, B.; Guo, Z.; Liu, S.; Zuo, G.; et al. Au-nanoparticle-supported ZnO as highly efficient photocatalyst for H₂O₂ production. *Catal. Commun.* **2020**, *134*, 105860. [[CrossRef](#)]
16. Kawano, S.; Fujishima, M.; Tada, H. Size effect of zinc oxide-supported gold nanoparticles on the photocatalytic activity for two-electron oxygen reduction reaction. *Catal. Commun.* **2020**, *144*, 106076. [[CrossRef](#)]
17. Xiong, X.; Zhang, X.; Liu, S.; Zhao, J.; Xu, Y. Sustained production of H₂O₂ in alkaline water solution using borate and phosphate-modified Au/TiO₂ photocatalysts. *Photochem. Photobiol. Sci.* **2018**, *17*, 1018–1022. [[CrossRef](#)]
18. Miah, M.R.; Ohsaka, T. Cathodic detection of H₂O₂ using iodide-modified gold electrode in alkaline media. *Anal. Chem.* **2006**, *78*, 1200–1205. [[CrossRef](#)]
19. Hirakawa, T.; Yawata, K.; Nosaka, Y. Photocatalytic reactivity for O₂^{·-} and OH[·] radical formation in anatase and rutile TiO₂ suspension as the effect of H₂O₂ addition. *Appl. Catal. A Gen.* **2007**, *325*, 105–111. [[CrossRef](#)]
20. Ma, X.; Li, H.; Liu, T.; Du, S.; Qiang, Q.; Wang, Y.; Yin, S.; Sato, T. Comparison of photocatalytic reaction-induced selective corrosion with photocorrosion: Impact on morphology and stability of Ag-ZnO. *Appl. Catal. B Environ.* **2017**, *201*, 348–358. [[CrossRef](#)]
21. Sahel, K.; Elsellami, L.; Mirali, I.; Dappozze, F.; Bouhent, M.; Guillard, C. Hydrogen peroxide and photocatalysis. *Appl. Catal. B Environ.* **2016**, *188*, 106–112. [[CrossRef](#)]
22. Skillen, N.; Ralphs, K.; Craig, D.; McCalmont, S.; Muzio, A.F.V.; O’Rourke, C.; Manyar, H.; Robertson, P. Photocatalytic Reforming of Glycerol to H₂ in a Thin Film Pt-TiO₂ Recirculating Photo Reactor. *J. Chem. Technol. Biotechnol.* **2020**, *95*, 2619–2627. [[CrossRef](#)]